Iodide impurities in hexadecyltrimethylammonium bromide (CTAB) products: lot-lot variations and influence on gold nanorod synthesis

Raja Gopal Rayavarapu,[†] Constantin Ungureanu,[†] Petra Krystek,[‡] Ton. G. van Leeuwen,[†,¶] and Srirang Manohar[*,†]

Biomedical Photonic Imaging, Faculty of Science and Technology, Mira Institute of Biomedical Technology and Technical Medicine, University of Twente, Postbox 217, 7500AE Enschede, The Netherlands,

MiPlaza Materials Analysis, Philips Research Europe, High Tech Campus 11, 5656 AE Eindhoven, The Netherlands, and

Biomedical Engineering and Physics, Academic Medical Center, University of Amsterdam, P.O. Box 22700, 1100 DE Amsterdam, The Netherlands

E-mail: s.manohar@utwente.nl

Abstract

Recent reports [Smith and Korgel, *Langmuir* 2008, 24, 644-649 and Smith et al., *Langmuir* 2009, 25, 9518-9524] have implicated certain hexadecyltrimethylammonium bromide (CTAB) products with iodide impurities, in the failure of a seed-mediated, silver and surfactant-assisted growth protocol, to produce gold nanorods. We used two of the three 'suspect' CTAB products and a 'good' CTAB product in the protocol, varying silver nitrate solutions in the growth

[*]To whom correspondence should be addressed
[†]University of Twente
[‡]Philips Research
[¶]University of Amsterdam

solutions. We obtained excellent gold nanorod samples as witnessed in signature longitudinal plasmon peaks in optical extinction spectra, which we substantiated using electron microscopy. Analysis of these samples using inductively coupled plasma mass spectroscopy (ICP-MS) failed to detect iodide. We subsequently learnt from discussions with Smith et al. that different lot numbers within the same product had been analyzed by our respective laboratories. We can conclude that iodide impurities can vary significantly from lot to lot within a product, to such an extent that there is no guarantee that gold nanorods can be synthesized with one or other CTAB product. Conversely, labelling a CTAB product, identified by a product number or supplier name, as one whose use precludes the formation of nanorods, is also hasty.

Introduction

Rod-shaped gold nanoparticles have attracted intense attention from researchers largely on two fronts:

1. in the biomedical physics arena where predominantly the plasmon resonance-driven optical features, especially intense absorptions in the near-infrared, inspire new ideas for applications in molecular medicine,[1–6]

2. in the fundamental chemistry and physics of underlying mechanisms of methods that initiate and nurture symmetry breaking of gold nuclei to form rods.[7–16]

This understanding in 2. is constantly evolving but as yet is not complete for synthesis protocols which may be described as working fairly well in their control of the size and shape of the nanoparticle products.[8,10,11,17] Basic scientific curiosity as to the mechanics at the atomic and molecular scales that culminate in the rod-shaped particles is not the only driving force for this research. A good understanding will provide a handle towards the desired exquisite and reproducible control over nanoparticle sizes and shapes, that will accelerate the transition of certain synthetic routes from laboratory protocols to manufacturing processes.

Recently the group of Smith and Korgel[18] published a study on the dependence of the success or failure of a well-accepted gold nanorod synthesis protocol,[10,19] on the source of hexadecyltrimethylammonium bromide (CTAB) used in the experiments. This study was initiated following their discovery[18,20] that certain CTAB products resulted only in nanosphere formation, while other products yielded nanorods as expected. The paper concluded that there was an undetermined impurity in certain CTAB products that disrupted the mechanism that produced nanorods. This impurity was subsequently identified as being iodide using inductively coupled plasma mass spectroscopy (ICP-MS).[21]

This intrigued us since we had used different CTAB products in synthesizing nanorods, always successfully.[22] We decided to test two of the three 'wrong' or 'suspect' CTABs (the third was not available from the supplier anymore) and a 'good' CTAB: Acros 22716V, Sigma H5882 and Fluka 52370 respectively. The synthesis procedure we used was similar to that described in Refs. 18 and 21. We found that we were able to synthesize excellent samples of nanorods from all three CTAB products. We then carefully analyzed the samples using inductively coupled plasma mass spectroscopy (ICP-MS), with methodological limits of detection superior to those in the aforementioned reports. No significant amounts of iodide were detected in any of the CTAB products.

Experimental

Protocol

We used, to the best of our understanding, the same protocol followed in Smith and Korgel[18] and Smith et al..[21] The only exception is that we use the growing gold spheres in the growth solution within 5 minutes, while Ref. 19 seeds growth solution after 2 hours. However, we do not believe this to be a crucial difference. The method is from Ref. 19 which itself is based on the seed-mediated silver-CTAB assisted protocol of Nikoobakht and El-Sayed.[10] We describe here the steps followed:

1. Preparation of growth solution: To freshly prepared 0.5 ml of 0.01 M gold salt solution, is

added 9.5 ml of 0.1 M CTAB solution with thorough mixing to yield a dark yellow solution. To this 55 μl of 0.1 M ascorbic acid is added with stirring. The resultant turns colorless. According to Ref. 19 a volume of between 20 - 100 μl of 0.01 M silver nitrate ($AgNO_3$) may be added to make the growth solution, but the Korgel group[21] appears to have specifically used 75 μl. We decided to use different volumes of 0.01 M $AgNO_3$ (20, 50, 70, 100, 200, 250, 300 and 350 μl), thus making 8 growth solutions which would be seeded in a subsequent step.

2. Preparation of gold seed: To freshly prepared 0.25 ml of 0.01 M gold salt solution, 9.75 ml of 0.1 M CTAB is added with stirring. Ice-cold, freshly prepared 0.01 M sodium borohydride solution in a volume of 0.6 ml is added to the mixture all at once with vigorous stirring for 2 minutes. The resultant is used within about 5 minutes to seed each growth solution.

3. Growth phase: The seed solution is added in a volume of 12 μl to the growth solutions with gentle stirring. The resultants are maintained undisturbed at 25^{o}C for 24 hours after which they are centrifuged and the supernatants removed. The precipitates are re-dispersed in 10 ml of water.

This procedure was repeated for each CTAB product tested.

Deliberate contamination of 'good' CTAB with potassium iodide

The protocol described above was followed using Fluka 52370 CTAB (see further) with the difference that two different volumes of 0.1 M potassium iodide (KI) were added to the growth solutions to obtain end-concentrations of 0.86 μM and 1.72 μM KI.

Materials and supplies

We used the following CTAB products: Acros 22716V, Sigma H5882 and Fluka 52370, for both growth and seed solutions. Of these the first two were 'wrong'[18,21] or 'suspect' CTAB, while the third was a 'good' CTAB.

Gold salt (Tetrachloroauric acid $HAuCl_4.3H_2O$, 99.99%) was purchased from Acros Organics (Belgium), sodium borohydride ($NaBH_4$, 99%), and ascorbic acid (99%) from Aldrich (The Netherlands), and silver nitrate ($AgNO_3$, 99.8%) from Merck (Germany). Solutions were prepared using Milli-Q Gradient System water (Millipore, Bedford, MA, USA). Prior to use, all glassware was cleaned with hydrofluoric acid (HF), further with aqua regia (HCl/HNO_3) and rinsed thoroughly with deionized water.

Materials characterization using ICP-MS

In addition to the CTAB samples above, we also studied Sigma H9151 as a second 'good' sample. The CTAB powders were weighed to 0.03 g in duplicate, and dissolved in 6 ml 2% nitric acid (HNO_3). To ensure dissolution of the samples, the vessels were placed in an ultrasonic bath for 15 minutes. The samples were then diluted 10-fold in an organic alkali: 2% tetra methyl ammonium hydroxide (TMAH) or tetraethyl ammonium hydroxide (TEAH) both from Fluka, were tested. Indium (In) was added off-line as the internal standard for drift compensation during the ICP-MS measurements. The final concentration in the analyzed solutions was 0.5 ppm In. The determination of iodide was carried out using a Perkin Elmer Elan 6100 DRC II ICP-MS.

The following operating conditions were used:
Forward RF power: 1450 W; Plasma gas flow: 15 L/min Ar; Auxiliary gas flow: 1.13 L/min Ar; Nebulizer gas flow: 0.90 L/min Ar. The isotopes ^{127}I and ^{115}In were measured using an integration time of 4.5 s, for five replicates. The calibration solutions were prepared from a stock standard solution from Perkin Elmer in the calibration range 0.25 to 1000 ppb I.

Nanoparticle characterization

Electron microscopy of the nanoparticles was performed using a Zeiss-1550 scanning electron microscope (SEM). Particle sizes were estimated using the NI Vision module (Labview, National Instruments) on the digital SEM images with around 200 particles considered in each case. In cases where the numbers of particles (rods or spheres) were low, the sizes were estimated using

the available numbers which are mentioned where size statistics are presented. (See Supporting Information.)

Optical transmission spectra (T vs. λ) of nanoparticles were measured with collimated transmission in a Shimadzu PC3101 UV-Vis-NIR spectrophotometer. Using the Beer-Lambert law, these were converted to extinction (μ_{ext} [mm^{-1}]) values as:

$$\mu_{ext}(\lambda) = \frac{1}{d} \ln \left\{ \frac{T(\lambda)}{100} \right\} \tag{1}$$

where d [mm] is the pathlength of the cuvettes used.

With the size and shape of the particles, ascertained from SEM and using Mie theory or Discrete Dipole Approximation (DDA)[23,24] for spheres and rods respectively, the optical extinction efficiency (Q_{ext}) of the nanoparticles was calculated. The concentration of particles was calculated as (See Supporting Information.):

$$N_{part}[\mathrm{cm}^{-3}] = \frac{\mu_{\mathrm{ext}}[\mathrm{cm}^{-1}]}{\mathrm{Q_{ext}} \pi \mathrm{r}^2 [\mathrm{cm}^2]} \tag{2}$$

where $r = (3V/4\pi)^{1/3}$ is the effective radius of a sphere having the same volume (V) as the particle.

Results

Nanoparticles using Acros 22716V CTAB

Figure 1(a) shows the optical extinction spectra of the 8 samples prepared using the different volumes of 0.01 M $AgNO_3$. Each spectrum's peak at 522 nm corresponds to the single plasmon peak of gold nanospheres and the transverse plasmon peak of gold nanorods. Each curve's reddened peak is the signature longitudinal plasmon peak of gold nanorods, incidently the biggest reason for the enormous interest in these particles for applications in molecular medicine as contrast agents for light[25] or light-excited therapeutic agents.[3]

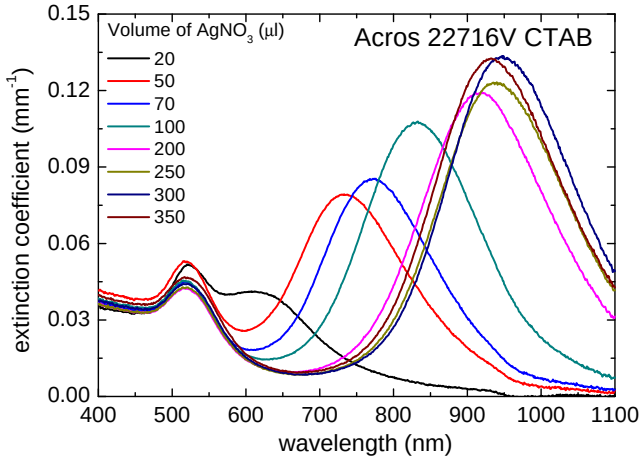

(a)

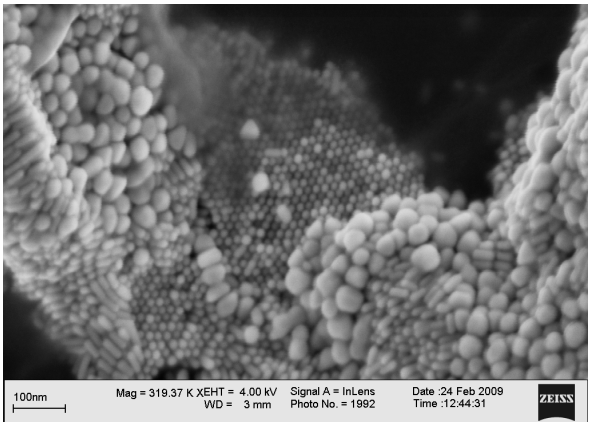

(b)

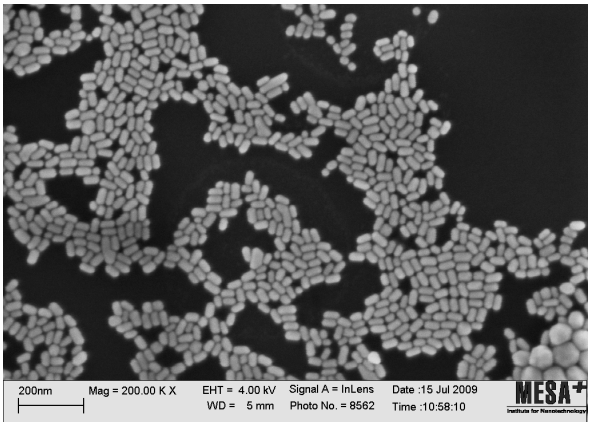

(c)

Figure 1: (a) Optical extinction spectra of gold nanoparticles synthesized when Acros 22716V CTAB was used. Red-shifted peaks in each spectrum indicate the presence of nanorods; all cases studied yielded nanorods with this CTAB. Scanning electron micrographs (SEM) of gold nanoparticles prepared when (b) 20 and (c) 50 μl of 0.01 M $AgNO_3$ were used respectively. In the former case, a relatively higher percentage of nanospheres are produced.

For the case of 20 μl $AgNO_3$, the relative amplitudes of the two peaks indicates that the sol contains a predominance of nanospheres compared with nanorods. From 50 μl $AgNO_3$ onwards, the situation is reversed with increasingly higher concentrations of nanorods. Beyond 300 μl $AgNO_3$, the red-shifting of the longitudinal plasmon peak and the increase in its amplitude appear to stop at 950 nm, with the last spectrum showing a slightly blue-shifted and lower amplitude peak.

Figure 1(b) and (c) are the SEM images of the particles produced using 20 and 50 μl $AgNO_3$. With the lowest volume of $AgNO_3$ there are indeed a higher proportion of spherical particles compared with nanorods.

Nanoparticles using Sigma H5882 CTAB

The extinction spectra in Figure 2 show the two signature peaks that betray gold nanorod presence, in all but the 20 μl 0.01 M $AgNO_3$ case; the solitary peak is due to gold nanospheres and no nanorods have been formed. With the use of 50 μl $AgNO_3$ a relatively higher proportion of gold spheres are present, but with progressively increasing Ag^+ ion concentrations, nanorods are formed in abundance. These are seen to possess higher aspect ratios with the red-shifting of the plasmon peaks until 850 nm for 250 μl $AgNO_3$. Beyond this there is regression with blue-shifting and lowering of amplitudes.

The SEM images corresponding to the cases 20, 50 and 250 μl $AgNO_3$ are seen in Figure 2(b), (c) and (d) which corroborate the spectral evidence for the relative absence or presence of gold nanorods in the three cases.

Nanoparticles using Fluka 52370 CTAB

The extinction spectra shown Figure 3 show a behaviour quite similar to the case with Acros, where nanorods are produced for all volumes of 0.01 M $AgNO_3$ used. Red-shifting however stops at 850 nm for 200 μl $AgNO_3$. It should be noted that the optical densities which correspond to the concentrations of particles in the sol, are higher in this case compared with when the Acros and Sigma CTAB products are used.

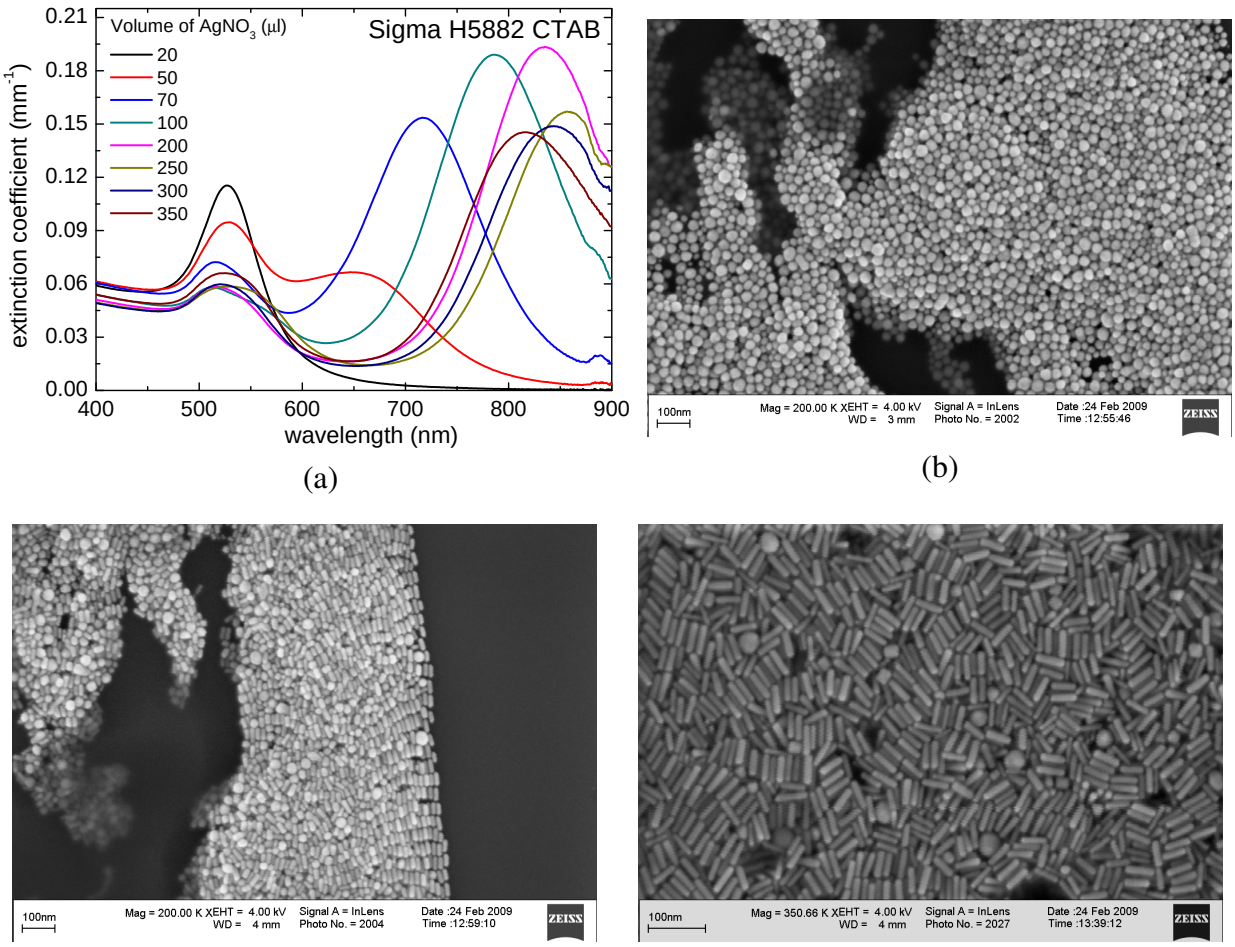

Figure 2: (a) Optical extinction spectra of gold nanoparticles synthesized when Sigma H5882 CTAB was used. Only for the case when 20 μl of 0.01 M $AgNO_3$ was used in the growth solution no nanorods were produced, as seen in the solitary peak at 522 nm signifying the presence of nanospheres. Scanning electron micrographs (SEM) of gold nanoparticles prepared with (b) 20 μl of $AgNO_3$ where only nanospheres were produced; (c) 50 μl of $AgNO_3$ where a relatively high percentage of nanospheres compared with nanorods were produced, and (d) 250 μl of $AgNO_3$ where a high percentage of nanorods were produced.

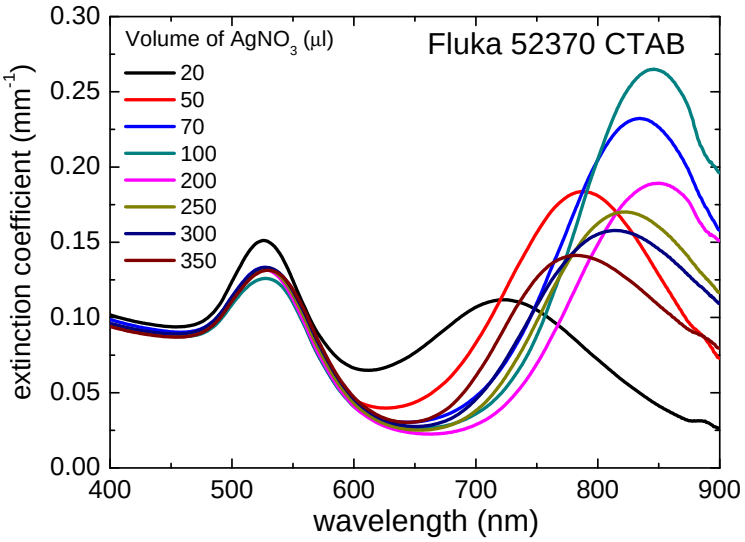

Figure 3: Optical extinction spectra of gold nanoparticles synthesized when Fluka 52370 CTAB was used. In all cases studied, nanorods were produced with this CTAB.

ICP-MS analysis of CTAB products

The results of several quality control experiments are summarized:

- Control of calibration range: The concentration of 25 ppb was controlled and the recovery was (n=1) 101% . The concentration of 100 ppb was controlled and the recovery was (n=1) 117%.

- Control of reference substance: Potassium iodide (KI) was used as reference substance. Two samples were pre-treated and measured according to the same procedure. The recovery was (n=2) 92.5±0.5%.

- Standard addition experiments to the CTAB matrix: Two recovery experiments by standard addition of a known concentration of iodide to the CTAB matrix were carried out and the recovery was (n=2) 101±6%.

Other tested variations of the procedure: Two experiments of the CTAB matrix were carried out by using a higher sample amount of 0.1 g. Nevertheless, this did not lead to significantly different results. Also the use of different organic alkalis (TMAH as well as TEAH) did not lead to significantly different results.

The methodological limit of detection (based on a weight of 0.03 g CTAB) was determined to be 0.5 ppm I. In all samples, whether 'good' or 'suspect', no significant amounts of iodide were detected.

Nanoparticles using Fluka 52370 CTAB deliberately contaminated with potassium iodide

Figure 4(a) shows the optical extinction spectrum for the particles produced with KI impurity in a concentration of 1.72 μM in the growth solution. The SEM image of the resulting particles is shown in Figure 4(b).

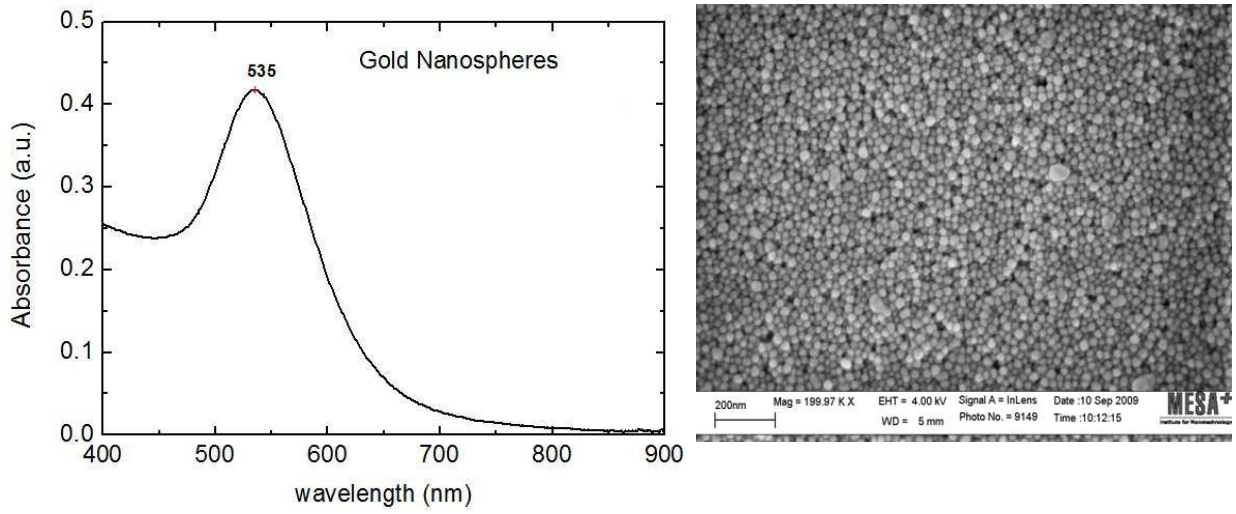

(a) (b)

Figure 4: For nanoparticles synthesized using growth solutions carrying 1.72 μM potassium iodide, (a) Optical absorbance spectrum showing the solitary plasmon peak indicative of gold nanospheres, (b) Scanning Electron Microscopy (SEM) image of the particles confirming presence of nanospheres and non-formation of nanorods.

Only gold spheres are obtained in this case. Similar results are obtained with KI concentration of 0.86 μM in the growth solution (not shown). These results are in agreement with the report of Smith *et al.*[21]

Discussion

We have synthesized excellent samples of gold nanorods using all three CTAB products including the two 'suspect' ones as shown in electron microscopy images and the optical spectra. The optical spectra may be described as being text-book curves with sharp peaks marking the wavelengths where the excited plasmons resonate along the length and width of the rod-shaped nanoparticles. The great sensitivity that nanorod sizes and consequently longitudinal plasmon peak positions, have for the Ag^+ ion concentrations in the growth solution are also evident (see Figs. 1(a), 2(a) and 3) using the different CTAB products. We have no doubt that the same physicochemical mechanisms responsible for the symmetry breaking in gold seed evolution and growth into nanorods dominate for all CTABs used with no evidence of disruption of the nanorod formation due to any impurities.

In sharp contradiction to Smith *et al*[21] we were unable to detect iodide impurities in the 'suspect' products. This finding concurs with the success of the nanorod synthesis protocol, when these CTAB products were used. When we deliberately contaminated the products with iodide, gold nanorod formation was indeed disrupted (Figure 4) corroborating the results of Smith *et al*.[21]

We are confident of the accuracy and reliability of our ICP-MS measurements which were performed with care after ensuring that several quality control checks had been successfully carried out. From discussions with the authors of Ref. 16 and 19, we learnt that the lot numbers analyzed by our two laboratories were different within the same CTAB product number. Table 1 consolidates our experiences and those of Smith *et al* with the various CTAB products. It is clear that there are significant variations in the presence of iodide impurities between the lots of the two 'suspect' CTABs, which implies that that the samples quantified by Smith *et al*[21] may be considered as different from the samples we studied even under the same product name.

It should be mentioned that even when nanorods are successfully synthesized, size reproducibility, manifested in variations in the optical properties across the CTAB products we studied leaves much to be desired. Figure 5(a) and (b) consolidate the outstanding differences between the nanorods produced using the various CTABs. An important difference is the threshold volumes

Table 1: Overview of results of gold nanorod synthesis, from this work and from Ref. 19, using various CTAB products with their iodide impurity concentrations measured using ICP-MS. The lot numbers of products used in Ref. 19 were obtained from the authors of the article.

supplier and purity	product number	lot numbers		nanorods		$[I^-]$(ppm)	
		ref. 19	this work	ref. 19	this work	ref. 19	this work
Acros $\geq 99\%$	22716	B0116374	A0258881	no	yes	57.68	< 0.5
Sigma $\geq 99\%$	H5882	055K0140	117K0732	no	yes	839.27	< 0.5
Fluka $\geq 96\%$	52370	445709 /110703248	43608036	yes	yes	< 2.75	< 0.5
Sigma $\sim 96\%$	H9151	095K0187	018K35291	yes	yes	< 2.75	< 0.5

of $AgNO_3$ required to produce nanorods. In the case with Sigma H5882, no nanorods are formed using 20 μl $AgNO_3$, in contrast with the other 2 cases. Further the amplitudes of the longitudinal plasmon peaks (Figure 5(a)) and their positions (Figure 5(b)) are different in the 3 cases.

It is possible that these variations are due to the modulation of the basic nanorod formation mechanism, by an interfering process as explained by Smith *et al*[21] due to the presence of iodide or other trace impurities which in our case are below the detectable limits. Also, while utmost care was taken, it is not possible to exclude variations in environmental conditions such as in ambient temperature etc, uncertainties in experimental conditions such as in seed aging times, in concentrations of components taken etc which could be affecting various steps in the trajectory followed for making the nanorods. These uncertainties would propagate in complex ways which could affect the final results.

One is also encouraged to resort to tweaking concentrations of various products added or fine-tune certain experimental conditions, to get the nanorod products that are desired. This is exemplified by a hypothetical situation, where had we stayed with the case of 20 μl $AgNO_3$ solution in combination with Sigma H5882 CTAB, perhaps we may have arrived at the same conclusion as Smith *et al*[21] and not decided to investigate the matter further.

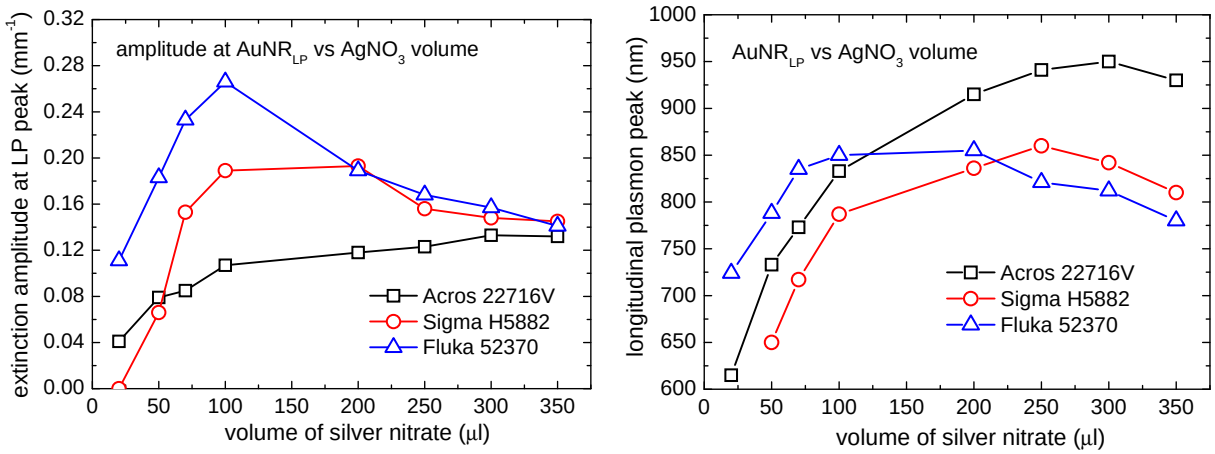

(a) (b)

Figure 5: Variation with respect to the volume of $AgNO_3$ used in the growth solutions of (a) the amplitude of the extinction coefficient at the longitudinal plasmon peak, and (b) the position of the longitudinal plasmon peak.

Conclusions

The most important conclusion is that iodide impurities can vary significantly from lot to lot within a CTAB product. It should not be a forgone conclusion that nanorods can or cannot be synthesized using certain CTAB products just based upon supplier name and product number; a lot number is required to make such judgements. Further, even with undetectable iodide impurities in CTAB products, variations in yields and dimensions of the nanorods produced across these products, points to possible influence of trace quantities of iodide or other impurities on the fundamental mechanism of nanorod formation. More research is required to identify contaminants and experimental conditions that can compromise reproducibility in gold nanorod synthesis.

Acknowledgement

The authors are grateful to Ms. C. Hermans (MiPlaza, Philips Research) for support during the analytical work. Dr. J. L. Hueso, Dr. D. K. Smith and Prof. B. A. Korgel (University of Texas at Austin) are thanked for their help in making their CTAB lot numbers available, and for sharing their experiences with lot-lot vagaries. The work is funded through the thrust area program NIMTIK of the University of Twente; through the PRESMITT project (IPD067771) of the SenterNovem

program IOP Photonic Devices; and by the Nederlandse Wetenschappelijk Organisatie (NWO) and Stichting Technische Wetenschappen (STW) through project TTF 6527.

References

(1) Huang, X.; El-Sayed, I. H.; Qian, W.; El-Sayed, M. A. *J. Am. Chem. Soc.* **2006**, *128*, 2115–2120.

(2) Liao, H.; Nehl, C. L.; Hafner, J. H. *Nanomedicine* **2006**, *1*, 201–208.

(3) Huang, X.; Jain, P. K.; El-Sayed, I. H.; El-Sayed, M. A. *Nanomed.* **2007**, *2*, 681–693.

(4) Pérez-Juste, J.; Pastoriza-Santos, I.; Liz-Marzán, L. M.; Mulvaney, P. *Coord. Chem. Rev.* **2005**, *249*, 1870 – 1901.

(5) Murphy, C. J.; Sau, T. K.; Gole, A. M.; Orendorff, C. J.; Gao, J.; Gou, L.; Hunyadi, S. E.; Li, T. *J. Phys. Chem. B* **2005**, *109*, 13857–13870.

(6) Li, P.-C.; Wang, C.-R. C.; Shieh, D.-B.; Wei, C.-W.; , C.-K. L.; Poe, C.; Jhan, S.; Ding, A.-A.; Wu, Y.-. *Opt. Exp.* **2008**, *16*, 18605–18615.

(7) Yu, Y.-Y.; Chang, S.-S.; Lee, S.-S.; Wang, C.-R. C. *J. Phys. Chem. B.* **1997**, *101*, 6661–6664.

(8) Jana, N. R.; Gearheart, L.; Murphy, C. J. *J. Phs. Chem. B* **2001**, *105*, 4065–4067.

(9) Nikoobakht, B.; El-Sayed, M. A. *Langmuir* **2001**, *17*, 6368–6374.

(10) Nikoobakht, B.; El-Sayed, M. A. *Chem. Mater.* **2003**, *15*, 1957–1962.

(11) Busbee, B. D.; Obare, S. O.; Murphy, C. J. *Adv. Mater.* **2003**, *15*, 414–416.

(12) Gole, A.; Murphy, C. J. *Chem. Mater.* **2004**, *16*, 3633–3640.

(13) Jiang, X.; Brioude, A.; Pileni, M. *Colloid. Surf. A* **2006**, *277*, 201 – 206.

(14) Liu, M.; Guyot-Sionnest, P. *J. Phys. Chem. B* **2005**, *109*, 22192–200.

(15) Grzelczak, M.; Pérez-Juste, J.; Mulvaney, P.; Liz-Marzán, L. M. *Chem. Soc. Rev.* **2008**, *37*, 1783 – 1791.

(16) Xia, Y.; Xiong, Y.; Lim, B.; Skrabalak, S. E. *Angew. Chem. Intl. Ed.* **2009**, *48*, 60–103.

(17) Grzelczak, M.; Sánchez-Iglesias, A.; Rodríguez-González, B.; Alvarez-Puebla, R.; Pérez-Juste, J.; Liz-Marzán, L. M. *Adv. Func. Mater.* **2008**, *18*, 3780–3786.

(18) Smith, D. K.; Korgel, B. A. *Langmuir* **2008**, *24*, 644–649.

(19) Gou, L.; Murphy, C. J. *Chem. Mater.* **2005**, *17*, 3668–3672.

(20) Durr, N. J.; Larson, T.; Smith, D. K.; Korgel, B. A.; Sokolov, K.; Ben-Yakar, A. *Nano Letters* **2007**, *7*, 941–945.

(21) Smith, D. K.; Miller, N. R.; Korgel, B. A. *Langmuir* **2009**, *25*, 9518–9524.

(22) Rayavarapu, R.; Petersen, W.; Ungureanu, C.; Post, J.; Van Leeuwen, T.; Manohar, S. *Int. J. Biomed. Imaging* **2007**, *29817*, 29817.

(23) Draine, B. T.; Flatau, P. J. *J. Opt. Soc. Am. A* **1994**, *11*, 1491–1499.

(24) Ungureanu, C.; Rayavarapu, R. G.; Manohar, S.; Van Leeuwen, T. G. *J. Appl. Phys.* **2009**, *105*, 102032–9.

(25) Eghtedari, M.; Oraevsky, A. A.; Copland, J. A.; Kotov, N. A.; Conjusteau, A.; Motamedi, M. *Nano Lett.* **2007**, *7*, 1914–1918.

Supporting Information: Gold nanorods, hexadecyltrimethylammonium bromide (CTAB) products and iodide impurities

Raja Gopal Rayavarapu[1], Constantin Ungureanu[1], Petra Krystek[2], Ton G. van Leeuwen[1,3] and Srirang Manohar[1,†]

[1]Biomedical Photonic Imaging, Faculty of Science and Technology, Mira Institute of Biomedical Technology and Technical Medicine, University of Twente, Postbox 217, 7500AE Enschede, The Netherlands

[2]MiPlaza Materials Analysis, Philips Research Europe, High Tech Campus 11, 5656 AE Eindhoven, The Netherlands

[3]Biomedical Engineering and Physics, Academic Medical Center, University of Amsterdam, P.O. Box 22700, 1100 DE Amsterdam, The Netherlands

1. Size distributions of nanoparticles produced

1.1. Using Acros 22716V

The Scanning Electron Microscopy (SEM) images of the particles produced using Acros 22716V are shown in Figures 2(b) and (c) in the manuscript. These are analyzed to ascertain size distributions.

1.2. Using Sigma H882

Figures 3(b), (c) and (d) (SEM images) in the manuscript are analyzed to ascertain size distributions. Table 1 consolidates the sizes of particles encountered in the images.

References

[1] D. K. Smith, N. R. Miller, and B. A. Korgel, "Iodide in CTAB prevents gold nanorod formation," *Langmuir* **25**, pp. 9518–9524, 2009.

† S.Manohar@utwente.nl

Table 1: Size distributions for samples prepared using the two 'suspect' CTAB products for different volumes of $AgNO_3$ used in the growth solutions. All dimensions of len (length), width and dia (diameter) are in nm; vol (volume) in μl; conc (concentration of nanorods) in NR/ml. Further, 'num' is number, 'NR' is nanorods and 'NS' is nanospheres.

CTAB product	$AgNO_3$ vol	NR length	NR width	aspect ratio	num of NR	NS size	num of NS	conc of NR
Acros	20	35.8±4.8	12.6±1.9	2.8±0.6	30	38±6.8	96	1×10^{10}
22716V	50	44±3.2	22±1.7	2.0±0.1	250	43±17.6	14	1.8×10^{10}
Sigma	20	N.A.	N.A.	N.A.	N.A.	25±3.2	250	N.A
H5882	50	33±3.2	15±1.7	2.1±0.2	180	26±5.5	83	1.6×10^{10}
	250	45±3.6	12±2.2	3.8±0.7	250	29±5.4	12	4×10^{10}